RAIL INSPECTION WITH GUIDED WAVES

J.L. Rose[1], C.M. Lee[1], T.R. Hay[2], Y. Cho[3], I. K. Park[4]

[1] Ultrasonics R&D Lab.,
Engineering Science and Mechanics Dept.,
The Pennsylvania State University, U.S
[2] FBS Co., State College, Pennsylvania, U.S
[3] School of Mechanical Engineering,
Pusan National University, Pusan, South Korea
[4] Department of Mechanical Engineering,
Seoul National University of Technology, Seoul, South Korea

Abstract

The critical subject of transverse crack detection in a rail head is treated in this paper. Conventional bulk wave ultrasonic techniques often fail because of shelling and other surface imperfections that shield the defects that lie below the shelling. A guided wave inspection technique is introduced here that can send ultrasonic energy along the rail under the shelling with a capability of finding the deleterious transverse crack defects. Dispersion curves are generated via a semi analytical finite element technique along with a hybrid guided wave finite element technique to explore the most suitable modes and frequencies for finding these defects. Sensor design and experimental feasibility experiments are also reported.

1. Introduction

Concern on nondestructive testing has increased over decades. Especially, the application of NDE to a mass transportation system such as a train is more essential since failure can cause a serious disaster. For this reason, many nondestructive testing methods have been developed as a consequence of a great effort of engineers and researchers. Ultrasonic testing using guided wave is a very promising technique because the guided wave can propagate long distance along the structure. Practical applications of guided waves for pipes were performed by Rose et al., Lowe et al., and Alleyne and Cawley[1-4]. The applications to the rail are also carried out by Rose, Cawley and Hayashi[5-8].

The numerous modes in a rail make it difficult to use of Normal Mode Expansion technique [9] in a practical testing. For this reason, a typical boundary value problem based on the wave mechanics is considered. The Finite Element Technique is used to solve this boundary value problem. In the rail industry, the numerous types of defects can be located in a rail. The shelling defects are usually located above the transverse crack and make it difficult to fine the transverse crack with traditional technique using Ultrasonics.

2. Problem Statement

Because of the arbitrary shape of a cross-section of a rail, the phase velocity dispersion curves can be calculated with the Semi-Analytical Finite Element (SAFE) technique [10]. *Figure 1* shows the phase velocity dispersion curves. It also displays the two calculation points where the wave scattering patterns are studied. The numerical model of the rail is modified to examine the influence of shelling. Initial geometries were taken from the report [11]. *Figure 2* shows the location and size of the defects and the shelling. The shapes of the defects are approximately rectangular with 0.1mm crack width. These defects are started 4mm under the top surface of the rail head. The half circle shaped shelling lies above the defect 1mm below the top surface of the rail head.

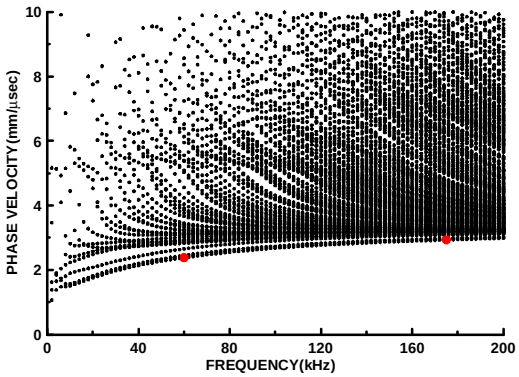

Figure 1 *Phase Velocity dispersion curves of a rail*

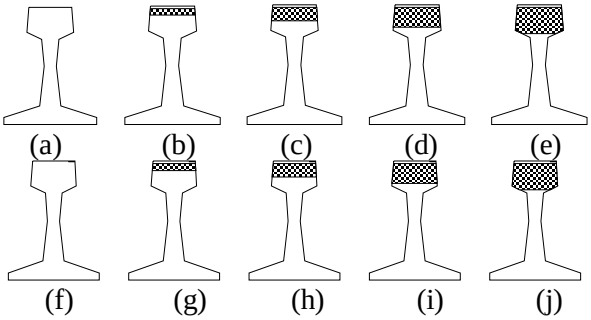

Figure 2 *Cross-section of the rail with shelling and various defects ((a):no defect, (b):10mm defect, (c):20mm defect, (d):30mm defect, (e):40mm defect, (f):shelling, (g):10mm defect with shelling, (h):20mm defect with shelling, (i):30mm defect with shelling, (j):40mm defect with shelling)*

3. Wave Scattering from Defects

The Lamb type EMAT transducers are simulated with an input signal of 60kHz and 175kHz. *Figure 3* shows the displacements of the reflected and transmitted waves at 185mm from the defect without the shelling ((a)-(e) in *Figure 2*) for the 60kHz case. The reflected wave from the bigger defect has the larger displacement and the transmitted wave from the smaller defect has the larger displacement.

The reflected waves in *Figure 3* are separated from the incident wave. However, it is difficult to distinguish the incident wave and reflected wave at the closed position from the crack. On the contrary, the transmitted waves are relatively clear. For this reason, the maximum value of the absolute value of U2 (vertical displacement of the rail) at several points for 60kHz and 175kHz are plotted in *Figure 4* and *Figure 5* respectively.

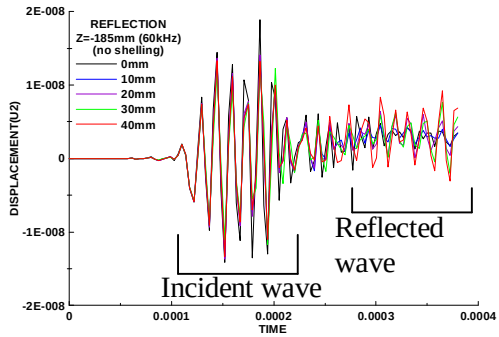

(a) Reflected waves

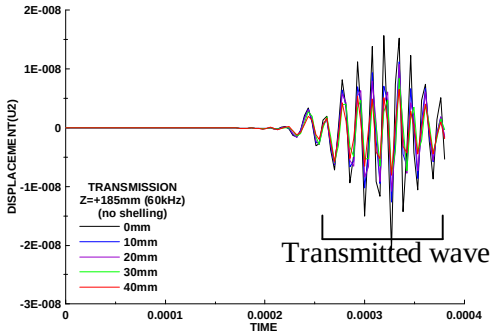

(b) Transmitted waves

Figure 3 *Reflected and transmitted waves at 185mm from the defect without shelling (60kHz)*

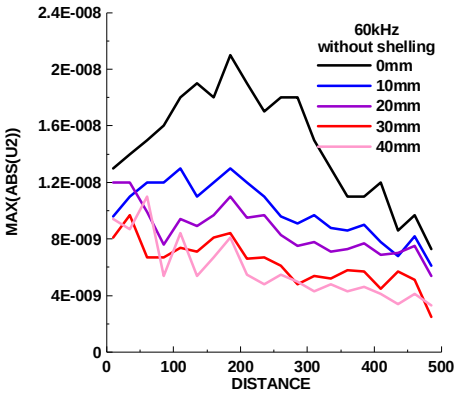

(a) |U2| without shelling

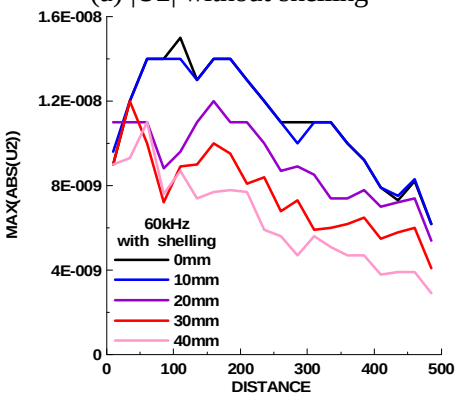

(b) |U2| with shelling

Figure 4 Absolute value of U2 of the transmitted wave at several points (60kHz)

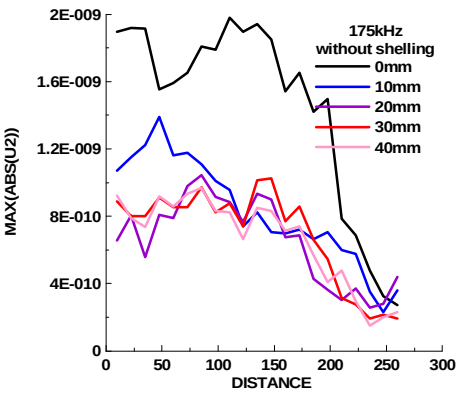

(a) |U2| without shelling

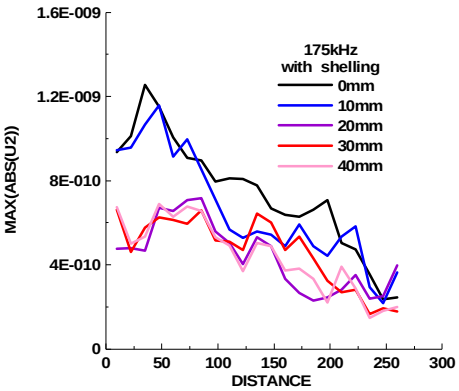

(b) |U2| with shelling

Figure 5 *Absolute value of U2 of the transmitted wave at several points (175kHz)*

In Figure 4, the magnitudes of |U2| between 150mm and 450mm are monotonically decreased with the crack depth. However, the amplitudes of no defect and 10mm defect with shelling are almost the same, because the size of the crack is relatively small. As shown in Figure 5 (a), the magnitude of |U2| between 100mm and 200mm shows a large difference between defects and no defect without shelling. On the contrary, the magnitude of |U2| in the same region shows no big difference between defects and no defect with shelling. Because the wave with higher frequency is closer to a surface wave and the shelling is treated as a defect.

3. Experimental Comfirmation

3.1 a hole in a clean rail head surface

The experiments for various types of artificial defects were performed in the Laboratory. To generate guided waves and to receive reflected waves from the defects, the Lamb type EMATs with four different frequencies (60kHz, 100kHz, 185kHz, and 280kHz) were used in a pulse-echo mode. The first specimen is a rail with a 0.25" diameter hole and a clean rail head surface. *Figure 6* shows the location of a hole in the rail. *Figure 7* shows the position of the hole and the EMAT locations. The guided waves are generated from the transmitter, passing the receiver directly, propagating along the rail, and then reflected from a hole or a rail end, and then arriving at the receiver again. Signals were obtained at different distances from a hole by moving the transmitter and the receiver. *Figure 8* shows the RF waveform at 18" from a hole as an example.

Unlike the numerical experiments, a received signal can be affected by many factors such as filtering, alignment of the EMATs, liftoff of the magnet of the EMAT, and the number of cycles used for input. Among them, the alignment of the EMATs is different when moved to new position. If the EMATs are misaligned, then both the direct signal and the reflected signal have small amplitudes. Therefore, the reflected signal from a defect is normalized with the direct signal. *Figure 9* shows the amplitude ratio of a reflected signal from a hole and a direct signal for a rail with a clean rail head surface with a hole at different positions. At a distance less than 1m, 60kHz and 100kHz guided waves have more potential for detecting the hole and after 1m, guided waves for four frequencies have a similar ability for detecting the hole.

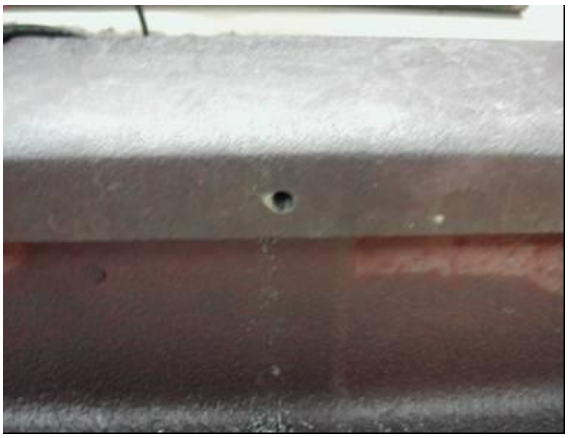

Figure 6 *A Photograph of a hole in a clean rail*

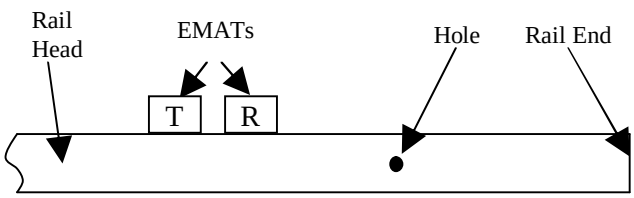

Figure 7 *The position of a hole and EMATs*

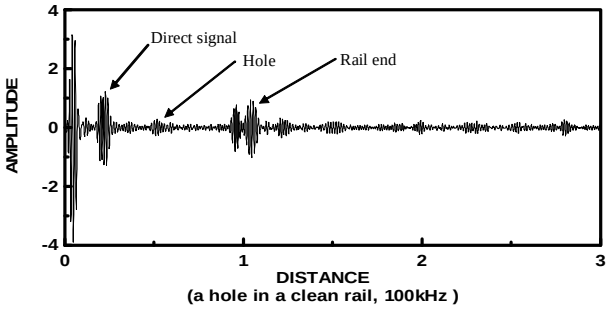

Figure 8 *RF wave form of a reflected wave from a hole in a clean rail for a 100kHz*

guided wave at a distance of 0.45m showing the direct signal, hole, and rail end.

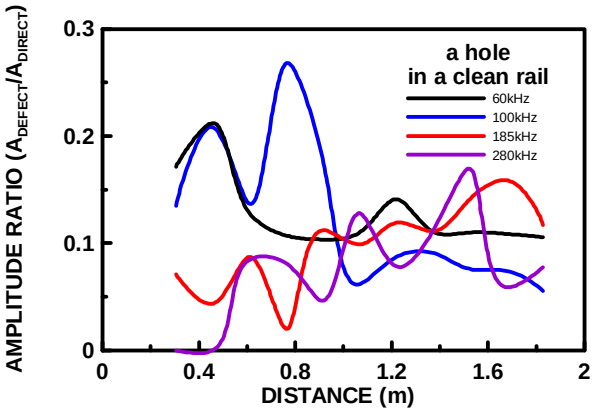

Figure 9 *Amplitude ratio for a rail with a clean surface of a rail head and a hole showing that at a distance less than 1m, 60kHz and 100kHz guided waves have more potential for detecting the hole*

3.2 a hole in a rough rail head surface

The third specimen is a rail with a rough rail head surface and a 0.25" diameter hole. It is shown in Figure 10. Figure 11 shows the amplitude ratio for a rail with a rail head rough surface and a hole at different positions. In this case, the guided waves for 280kHz cannot detect a hole over the entire distance since a collection of small echoes from the rough surface does not allow any energy to reach the defect. On the contrary, guided waves for lower frequencies (60kHz and 100kHz) can find the hole.

Figure 10 *A Photograph of a hole in a rough rail*

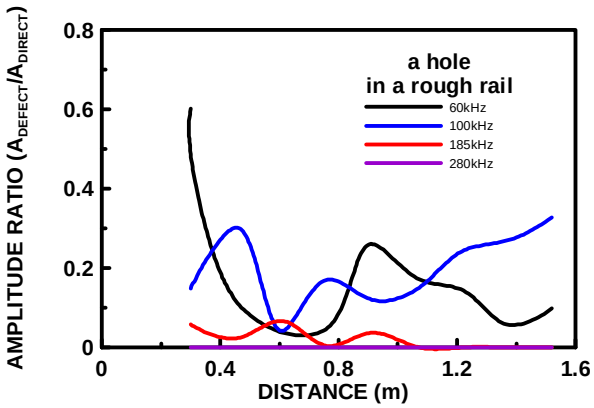

Figure 11 *Amplitude ratio for a rail with a rough rail head surface and a hole showing that guided waves for 60kHz and 100kHz can find the hole, 185kHz is marginal, and the 280kHz guided wave cannot see the hole since a collection of small echoes from the rough surface does not allow any energy to reach the defect*

4. Conclusions

In this paper, the Lamb type EMAT transducers are simulated using Finite Element technique. The characteristics of scattering from defects and shelling are also explored. The absolute values of U2 (vertical displacement of the rail) of transmitted waves are monotonically decreased with the crack depth for 60kHz Lamb wave. For 175kHz Lamb wave can not distinguish the shelling and the crack. The absolute values of U2 of transmitted waves show the big difference between defects without shelling and no defect without shelling for 175kHz Lamb waves.

The experiments for hole defect in a clean and rough rail were performed in the Laboratory. To generate guided waves and to receive reflected waves from the defects, the Lamb type EMATs with four different frequencies (60kHz, 100kHz, 185kHz, and 280kHz) were used in a pulse-echo mode. The guided waves with higher frequency (185kHz and 280kHz) are sensitive to the surface roughness of the rail head because the most of energy is concentrated in the top surface of the rail head.

Therefore, the best condition in detecting a transverse defect under a shelling is the guided waves with lower frequencies (60kHz and 100kHz).

5. References

[1] J. L. Rose, J. J. Ditri, A. Pilarski, J. Zhang, F. T. Carr, and W. J. McNight, "A Guided Wave Inspection Technique for Nuclear Steam Generator Tubing", *Nondestr. Test*. 92, 191-195, 1992

[2] J. L. Rose, K. M. Rajana, and F. T. Carr, "Ultrasonic Guided Wave Inspection Concepts for Steam Generator Tubing*," Mater. Eval*. 52(2), 307-311, 1994

[3] M.J.S. Lowe, D.N. Alleyne and P. Cawley, "The Mode Conversion of a Guided Wave by a Part-Circumferential Notch in a Pipe*", J. Appl. Mech*., 65, 211-214, 1998

[4] D.N. Alleyne and P. Cawley, "Long Range Propagation of Lamb Waves in Chemical Plant PipeWork", *Materials Evaluation*, 55, 504-508, 1997

[5] J.L. Rose, M.J. Avioli and W.-J. Song, "Application and potential of guided wave rail inspection", *Insight*, 44(6), 353-358, 2002

[6] J.L. Rose, M.J. Avioli and Younho Cho, "Elastic Wave Analysis for Broken Rail Detection", *Review of Quantitative Nondestructive Evaluation*, 21, 1806-1812, 2002

[7] P. Cawley, M.J.S. Lowe, D.N. Alleyne, B. Pavlakovic and P. Wilcox, "Practical Long Range Guided Wave Testing : Application to Pipes and Rails", *Materials Evaluation*, 61(1), 66-74, 2003

[8] T. Hayashi, W.-J. Song and J.L. Rose, "Guided Wave Dispersion Curves for a Bar with an Arbitrary Cross-Section, a Rod and Rail Example", *Ultrasonics*, 41, 175-183, 2003

[9] Y. Cho and Joseph L. Rose, A Boundary Element Solution for a Mode Conversion Study on the Edge Reflection of Lamb Waves, *J. Acoust. Soc. Am.* Vol. 99(4) (1996) p.2097-2109

[10] Takahiro Hayashi, Won-Joon Song, and Joseph L. Rose, Guided wave dispersion curves for a bar with an arbitrary cross-section, a rod and rail example, *Ultrasonics*, Vol. 41 (2003), p.175-183

[11] Flaw Characterization of Rail Service Failures, *Report No. R-963 AAR Research Report July 2003*

Acknowledgement

Thanks are given to the Federal Railroad Administration for their support of this work. Thanks are also given to Mike Avioli at FBS. Inc. for his assistance.